

Field-induced slow magnetic relaxation in two interpenetrated cobalt(II) metal-organic framework isomers

Xiao-Qin Wei,^{*a} Dong Shao,^b Cai-Long Xue,^a Xing-Yu Qu,^a Jie Chai,^a Jian-Qing Li,^a Yi-En Du,^a and Yong-Qiang Chen^{*a}

^a Department of Chemistry and Chemical Engineering, Jinzhong University, Jinzhong, 030619, China.

^b State Key Laboratory of Coordination Chemistry, School of Chemistry and Chemical Engineering, Nanjing University, Nanjing, 210023, China.

* chenyongqiang@jzxy.edu.cn

* weixiaoqin@jzxy.edu.cn

Table of Content	
Experimental Section	3
Table S1. Crystallographic data and structure refinement parameters for 1 and 2	5
Table S2. Selected bond lengths (Å) and angles [°] for 1	6
Table S3. Selected bond lengths (Å) and angles [°] for 2	7
Figure S1. Comparison of the experimental PXRD patterns of 1 and 2 with the simulated patterns from their single crystal structures.	8
Figure S2. Square Co ₄ units of 1	9
Figure S3. A side view of the double-interpenetrated two-layer interwoven of 1	10
Figure S4. The packing structure of 1	11
Figure S5. The 3D packing structure of 1	12
Figure S6. Hexagonal diamondoid Co ₆ unit of 1	13
Figure S7. Thermal gravimetric analysis (TGA) curves of 1 and 2	14
Figure S8. N ₂ adsorption (open symbol) and desorption (filled symbol) isotherms for 1 and 2 measured at 77 K.....	15
Figure S9. Frequency dependence of the in-phase (χ') and out-of-phase (χ'') ac susceptibilities measured under zero dc field at 1.8 K for 1 and 2	16
Figure S10. Temperature dependence of the in-phase (χ') and out-of-phase (χ'') ac susceptibilities measured under 1000 Oe dc field at 1.8 K for 1 and 2	17
Figure S11. a) Cole-cole plot for 2 under 1 kOe dc field. b) Arrhenius plot with $\ln(\tau)$ versus T^{-1} for 2 . The red and blue lines represent the results using Orbach and multiple Raman and QTM relaxation mechanism, respectively.....	18
Table S4. Relaxation fitting parameters from the least-square fitting of the Cole-Cole plots of 1 according to the generalized Debye model.	19
Table S5. Relaxation fitting parameters from the least-square fitting of the Cole-Cole plots of 2 according to the generalized Debye model.	20

Experimental Section

Materials and Synthesis

1H-benzimidazole-5-carboxylic acid were purchased from commercially available sources and used without further purification. All other reagents are commercially available and used as purchased.

Synthesis of [Co(Hbic)₂]_α (1)

Co(NO₃)₂·6H₂O (0.1 mmol, 29.1 mg), H₂bic (0.1 mmol, 16.2 mg), and 4 ml of mixed DMF/MeOH (1:2) solvent were placed in a 15 mL Pyrex glass tube, then heated in an oven at 90 °C for three days. The reaction system was gradually cooled to room temperature. After two days, single-phase blue single crystals were obtained. Yield: ~22 mg, ca. 58% (based on Co(NO₃)₂·6H₂O). Elemental analysis calcd. (%) for C₁₆H₁₀CoN₄O₄: C, 50.41; H, 2.64; N, 14.69. Found: C, 50.19, H, 2.53; N, 14.48. IR (KBr, cm⁻¹): 3451 (bs), 1632 (s), 1604(s), 1578(s), 1493(s), 1407 (m), 1382 (s), 967 (w), 777 (m), 670 (w), 539 (w) cm⁻¹.

Synthesis of [Co(Hbic)₂]_β (2)

A mixed reaction system containing Co(NO₃)₂·6H₂O (0.1 mmol, 29.1 mg), H₂bic (0.2 mmol, 32.4 mg), and 4 ml ethanol was placed in a 15 mL Pyrex glass tube, and keep stirring the mixed solution for one hour, then heated in an oven at 120 °C for three days. After cooling naturally to room temperature, block blue single crystals formed. Yield: ~78 mg, ca. 35% (based on Co(NO₃)₂·6H₂O). Elemental analysis calcd (%) for C₁₆H₁₀CoN₄O₄: C, 50.41; H, 2.64; N, 14.69. Found: C, 50.26, H, 2.76; N, 14.52. IR (KBr, cm⁻¹): 3450 (bs), 1620 (s), 1530 (s), 1417 (m), 1382 (s), 968 (w), 767 (m), 671 (w), 540 (w) cm⁻¹.

Physical Measurements

Infrared spectra (IR) data were measured on KBr pellets using a Nexus 870 FT-IR spectrometer in the 4000-400 cm⁻¹ range. Elemental analyses of C, H, and N were performed at an Elementar Vario MICRO analyzer. Thermal gravimetric analysis (TGA) was measured in Al₂O₃ crucibles using a PerkinElmer Thermal Analysis in the temperature range of 20-650 °C under flowing nitrogen at a heating rate of 20 °C/min. Powder X-ray diffraction data (PXRD) were recorded at 298 K on a Bruker D8 Advance diffractometer with Cu K α X-ray source ($\lambda = 1.5405 \text{ \AA}$) operated at 40 kV and 40 mA. Magnetic measurements were collected using Quantum Design SQUID VSM magnetometer on crushed single crystals. Direct current (dc) magnetic susceptibility measurements were performed in the temperature range of 2-300 K under an applied dc field of 1000 Oe. Alternative current (ac) susceptibility measurements were performed with a 2 Oe ac oscillating field in an operating frequency range of 1-1000 Hz under various dc fields. Magnetization data were collected in the 0 to 70 kOe field range. Experimental susceptibilities were corrected for diamagnetism of the sample holders and that of the compounds according to Pascal's constants.

X-ray Crystallography

Single crystal X-ray crystallographic data were collected on a Bruker APEX D8 QUEST diffractometer with a Photon 100 CMOS detector (Mo-K α radiation, $\lambda = 0.71073 \text{ \AA}$). The APEX III program was used to determine the unit cell parameters and for data collection. The data were integrated and corrected for Lorentz and polarization effects using SAINT.^{S1} Absorption corrections were applied with SADABS.^{S2} The structures were solved by direct method and refined by full-

matrix least-squares method on F^2 using the SHELXTL software package.^{S3} All the non-hydrogen atoms were refined anisotropically. Hydrogen atoms of the organic ligands were refined as riding on the corresponding non-hydrogen atoms. Additional details of the data collections and structural refinement parameters were provided in Table 1. Selected bond lengths and bond angles of **1** and **2** were listed in Table S1. CCDC-2014292, 2014293 for compounds **1** and **2**, respectively, contain the supplementary crystallographic data for this paper. These data can be obtained free of charge from The Cambridge Crystallographic Data Centre via www.ccdc.cam.ac.uk/data_request/cif.

Table S1. Crystallographic data and structure refinement parameters for **1** and **2**.

Complex	1	2
Formula	C ₁₆ H ₁₀ CoN ₄ O ₄	C ₁₆ H ₁₀ CoN ₄ O ₄
Formula Weight	381.21	381.21
Crystal system	Monoclinic	Orthorhombic
Space group	P2 ₁ /n	Pna21
<i>a</i> [Å]	7.679(4)	14.8116(8)
<i>b</i> [Å]	24.128(11)	8.7686(4)
<i>c</i> [Å]	9.496(4)	14.8164(7)
α [°]	90	90
β [°]	113.85	90
γ [°]	90	90
<i>V</i> [Å ³]	1609.2(13)	1924.31(16)
<i>Z</i>	4	4
<i>T</i> [K]	150(2)	296(2)
ρ_{calcd} [g cm ⁻³]	1.574	1.316
$\mu(\text{Mo-K}\alpha)$ [mm ⁻¹]	1.096	0.916
<i>F</i> (000)	772	772
Refl. collected / unique	6340 / 2742	32689 / 9809
<i>R</i> _{int}	0.0864	0.0632
<i>R</i> ₁ ^a / <i>wR</i> ₂ ^b (<i>I</i> > 2σ(<i>I</i>))	0.0710 / 0.1618	0.0639 / 0.1737
<i>R</i> ₁ / <i>wR</i> ₂ (all data)	0.1155 / 0.1783	0.0993 / 0.1947
GOF on <i>F</i> ²	0.964	1.157
Max/min [e Å ⁻³]	0.9472 / 0.8271	1.435 / -0.604

$$^a R_1 = \frac{\sum ||F_o| - |F_c||}{\sum |F_o|} \quad ^b wR_2 = \left\{ \frac{\sum [w(F_o^2 - F_c^2)^2]}{\sum [w(F_o^2)]} \right\}^{1/2}$$

Table S2. Selected bond lengths (Å) and angles [°] for **1**.

Co(1)-O(1)	1.974(4)
Co(1)-O(2)	1.958(4)
Co(1)-N(1)#2	2.019(4)
Co(1)-N(3)#1	2.001(5)
Co-N/O	1.988
O(2)-Co(1)-O(1)	104.87(17)
O(2)-Co(1)-N(3)#1	100.49(19)
O(1)-Co(1)-N(3)#1	108.93(19)
O(2)-Co(1)-N(1)#2	116.36(19)
O(1)-Co(1)-N(1)#2	123.88(17)
N(3)#1-Co(1)-N(1)#2	99.5(2)

Symmetry transformations used to generate
equivalent atoms:

#1 $x-1/2, -y+3/2, z+1/2$; #2 $x-1, y, z-1$; #3

$x+1, y, z+1$

Table S3. Selected bond lengths (Å) and angles [°] for **2**.

Co(1)-O(1)	1.996(3)
Co(1)-O(2)	1.994(4)
Co(1)-N(1)#2	2.029(5)
Co(1)-N(3)#1	2.083(6)
Co-N/O	2.026
O(1)-Co(1)-O(2)	134.61(12)
O(1)-Co(1)-N(3)#1	100.54(17)
O(2)-Co(1)-N(3)#1	107.84(18)
O(1)-Co(1)-N(1)#2	108.18(16)
O(2)-Co(1)-N(1)#2	101.03(17)
N(3)#1-Co(1)-N(1)#2	99.9(2)

Symmetry transformations used to generate
equivalent atoms:

#1 $x-1/2, -y+5/2, z$; #2 $-x+1, -y+1, z-1/2$; #3 $-x+1, -y+1, z+1/2$

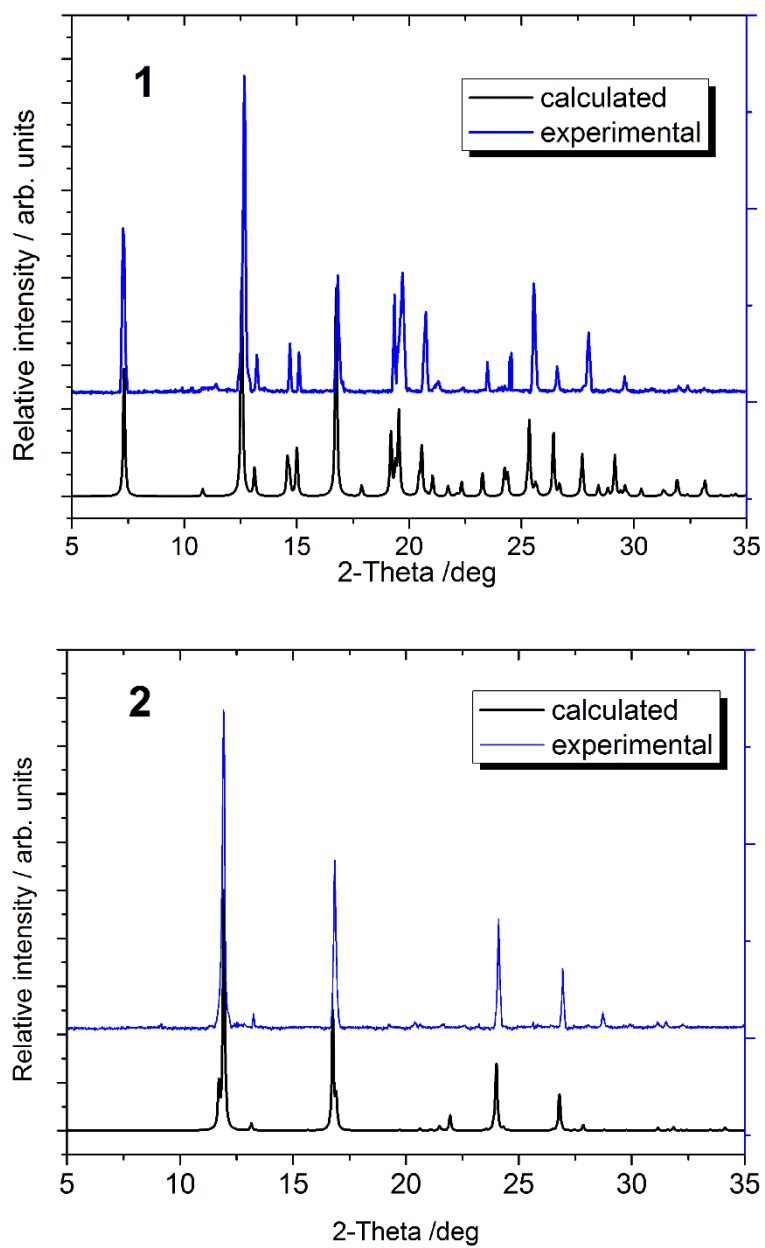


Figure S1. Comparison of the experimental PXRD patterns of **1** and **2** with the simulated patterns from their single crystal structures.

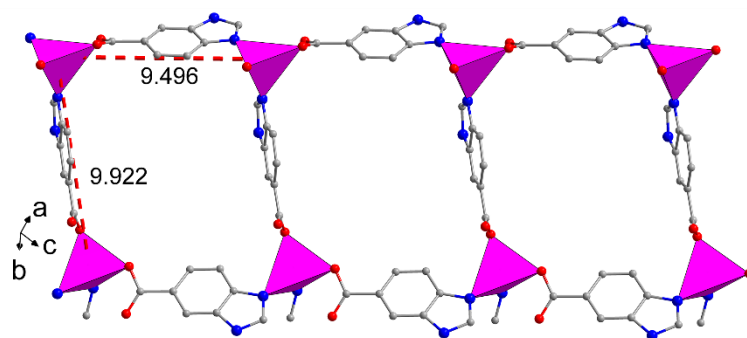


Figure S2. Square Co_4 units of **1**.

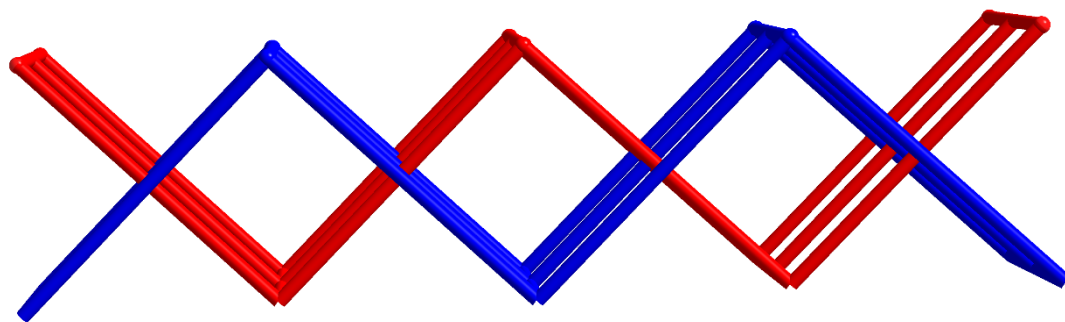


Figure S3. A side view of the double-interpenetrated two-layer interwoven of **1**.

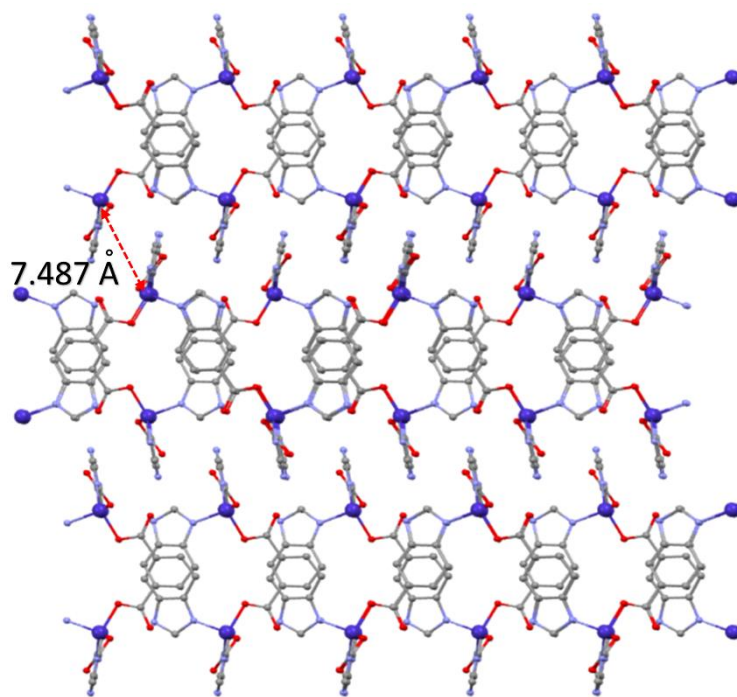


Figure S4. The packing structure of **1**.

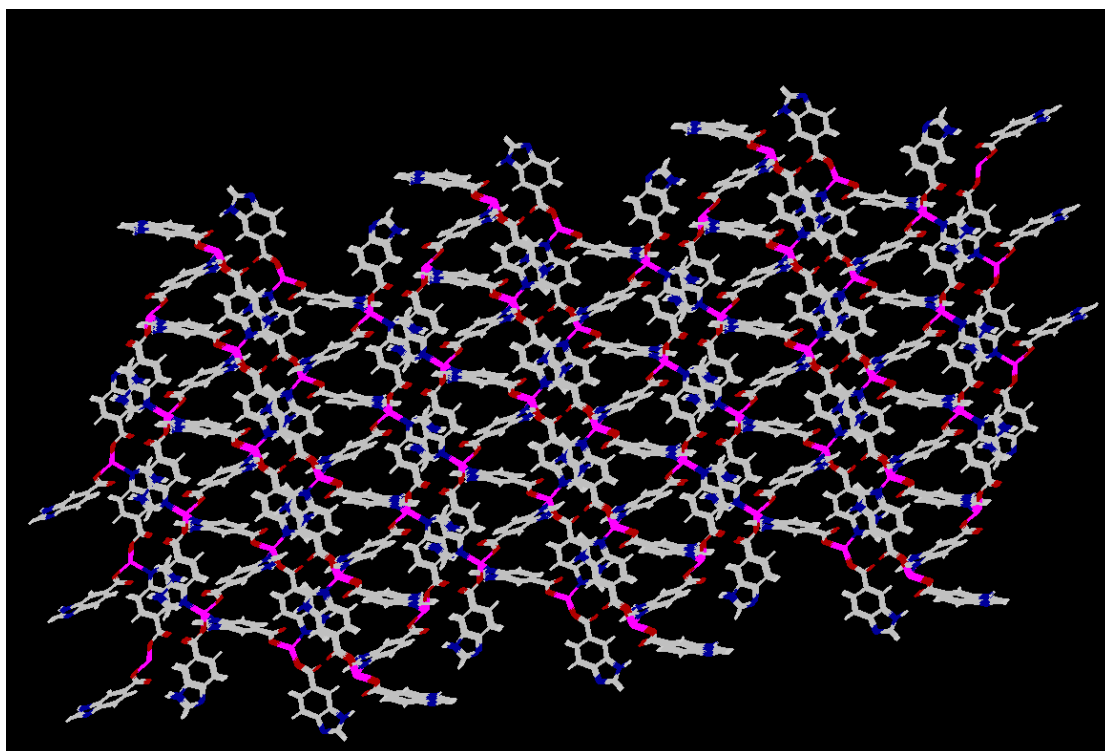


Figure S5. The 3D packing structure of **1**.

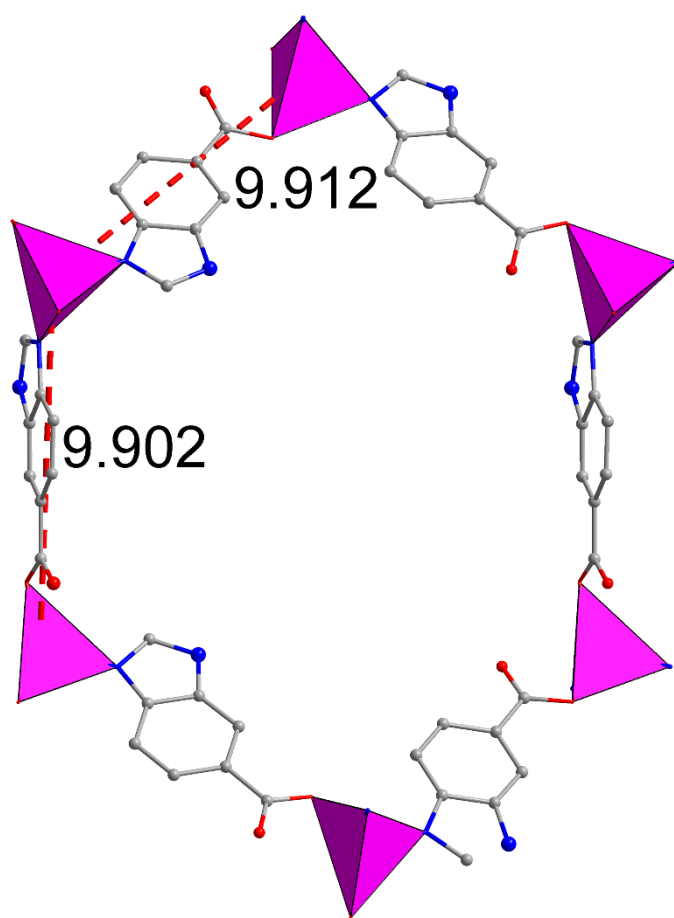


Figure S6. Hexagonal diamondoid Co₆ unit of **1**.

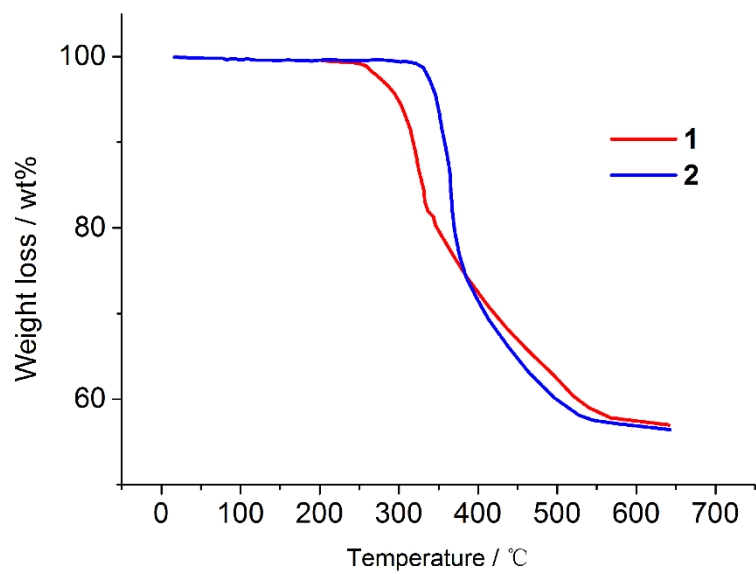


Figure S7. Thermal gravimetric analysis (TGA) curves of 1 and 2.

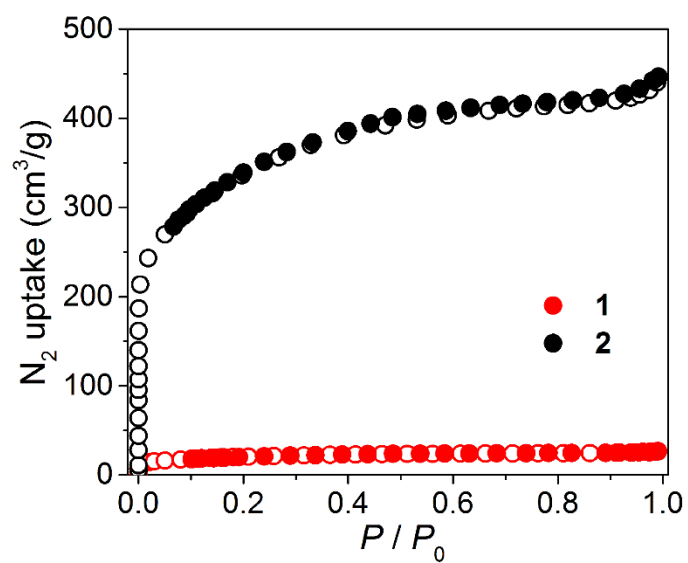


Figure S8. N₂ adsorption (open symbol) and desorption (filled symbol) isotherms for **1** and **2** measured at 77 K.

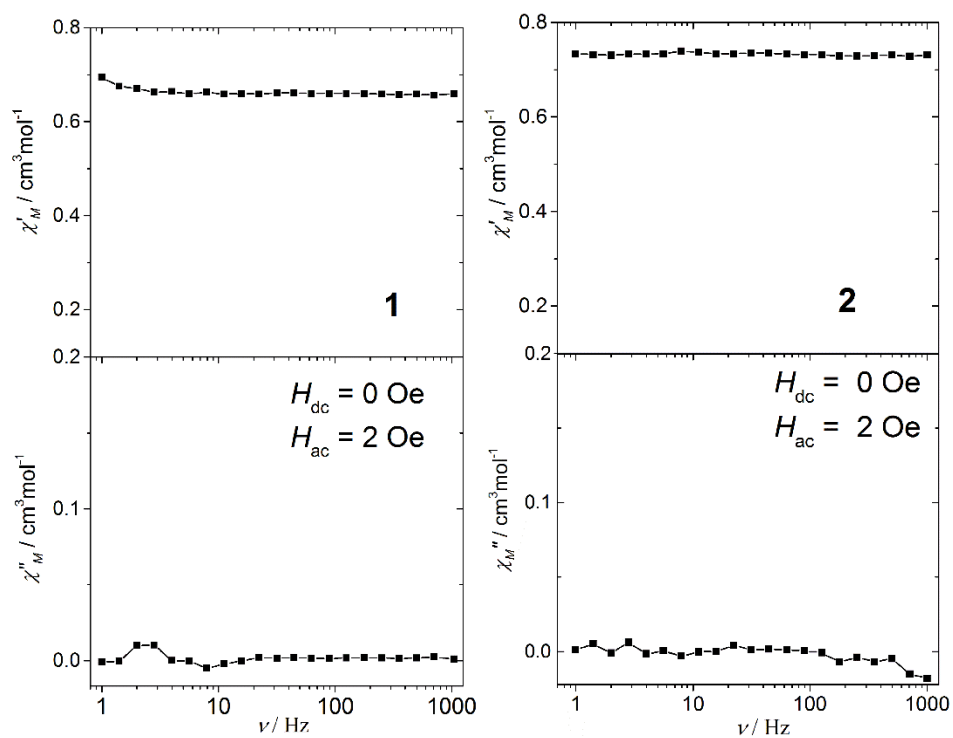


Figure S9. Frequency dependence of the in-phase (χ') and out-of-phase (χ'') ac susceptibilities measured under zero dc field at 1.8 K for **1** and **2**.

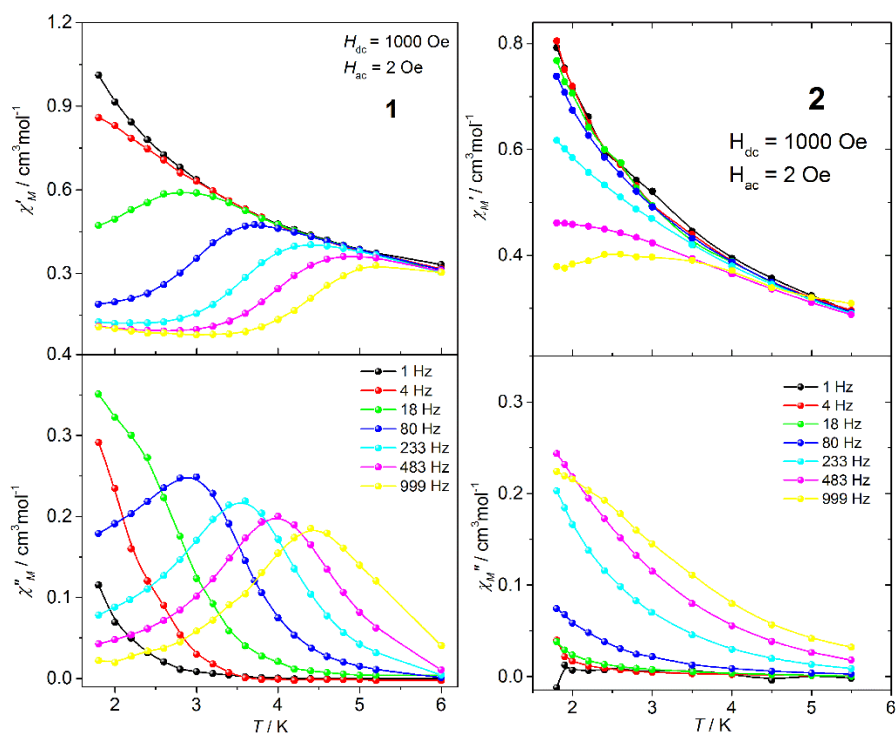


Figure S10. Temperature dependence of the in-phase (χ') and out-of-phase (χ'') ac susceptibilities measured under 1000 Oe dc field at 1.8 K for **1** and **2**.

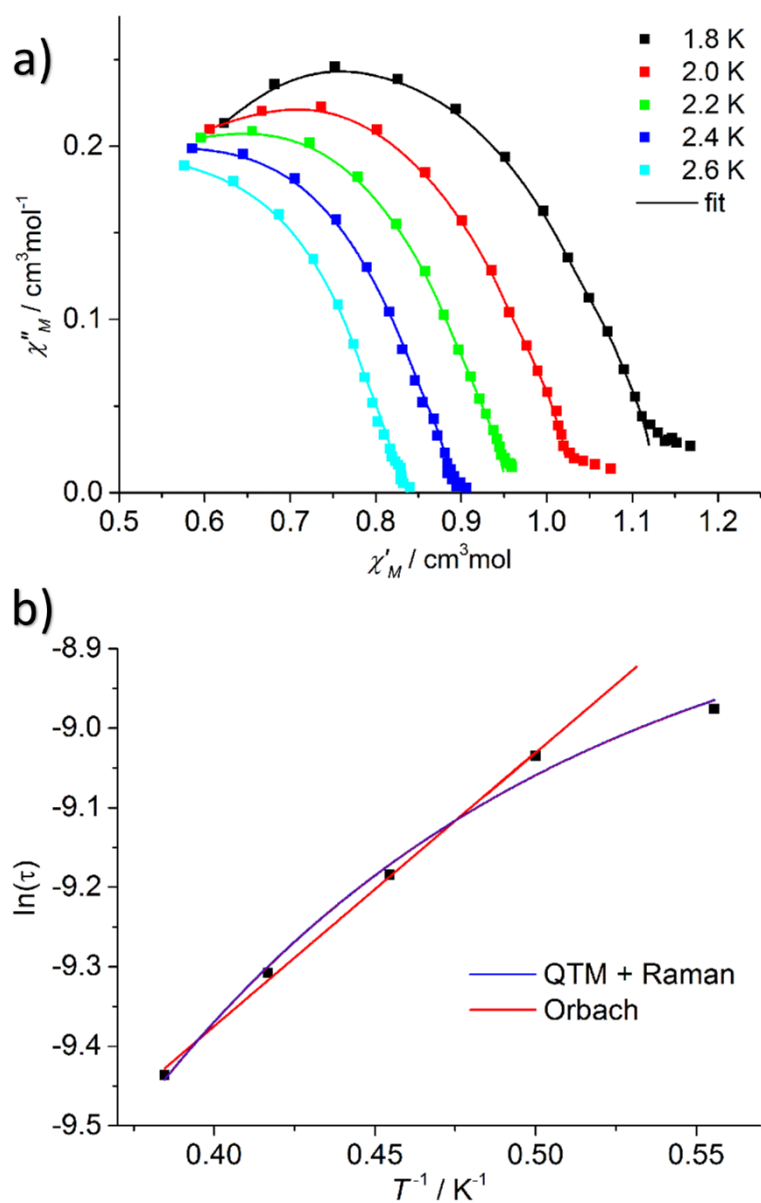


Figure S11. a) Cole-cole plot for **2** under 1 kOe dc field. b) Arrhenius plot with $\ln(\tau)$ versus T^{-1} for **2**. The red and blue lines represent the results using Orbach and multiple Raman and QTM relaxation mechanism, respectively.

Table S4. Relaxation fitting parameters from the least-square fitting of the Cole-Cole plots of **1** according to the generalized Debye model.

T / K	$\chi_S / \text{cm}^3\text{mol}^{-1}\text{K}$	$\chi_T / \text{cm}^3\text{mol}^{-1}\text{K}$	τ / s	α
1.8	0.08391	0.85958	0.00699	0.15542
2	0.07856	0.79223	0.00529	0.14116
2.2	0.07746	0.73346	0.00387	0.11196
2.4	0.07154	0.67975	0.00278	0.10063
2.6	0.06978	0.63618	0.00198	0.07703
2.8	0.06475	0.59862	0.00141	0.0703
3.0	0.06306	0.56245	9.94271E-4	0.0515
3.2	0.06413	0.53174	7.14501E-4	0.03375
3.4	0.06084	0.50469	5.10352E-4	0.03136
3.6	0.05787	0.48095	3.67972E-4	0.03073
3.8	0.0572	0.45718	2.69308E-4	0.02121
4.0	0.0478	0.43822	1.9366E-4	0.02973
4.2	0.03242	0.41998	1.36412E-4	0.04304

Table S5. Relaxation fitting parameters from the least-square fitting of the Cole-Cole plots of **2** according to the generalized Debye model.

T / K	$\chi_S / \text{cm}^3\text{mol}^{-1}\text{K}$	$\chi_T / \text{cm}^3\text{mol}^{-1}\text{K}$	τ / s	α
1.8	3.22727E-12	0.90026	1.26458E-4	2.7019E-11
2	4.01348E-12	0.96709	1.19197E-4	3.30295E-11
2.2	4.68878E-12	0.89977	1.02648E-4	5.31561E-11
2.4	6.2723E-12	0.84776	9.07241E-5	7.43708E-11
2.6	8.16961E-12	0.79563	7.97887E-5	1.12099E-10
1.8	3.22727E-12	0.90026	1.26458E-4	2.7019E-11

Reference:

- S1. SAINT Software Users Guide, version 7.0; Bruker Analytical Xray Systems: Madison, WI, 1999.
- S2. Sheldrick, G. M. SADABS, version 2.03; Bruker Analytical X-ray Systems: Madison, WI, 2000.
- S3. Sheldrick, G. M. SHELXTL, version 6.14; Bruker AXS, Inc.: Madison, WI, 2000–2003.